BEAM PARAMETERS MEASUREMENT OF TECHNOLOGICAL 10 MEV LINAC*

A.S. Alimov, E.A. Alimov, A.N. Kamanin, V.V. Khankin, N.I. Pakhomov, V.I. Shvedunov[#], SINP MSU, 119992 Moscow, Russia

A.V. Gryzlov, S.V. Lamonov, A.P. Musatov, V.N. Sigalaev, FSUE RPC "Toriy", Moscow, Russia.

Abstract

Prototype of technological electron linac with beam energy 10 MeV has been designed and built in collaboration of SINP MSU and FSUE RPC "Toriy" [1]. We describe here methods and results of the beam parameters measurement and compare the results with calculations.

INTRODUCTION

10 MeV standing wave technological linac has been designed to provide electron beam with an average power varying from 4 to 45 kW depending on a RF source average power. During the linac commissioning the main beam parameters: pulsed and average current, energy spectrum, beam spot dimensions were measured at special stand. Here we shortly characterize the linac, describe methods and results of the beam parameter measurements, compare the measured results with calculations.

ACCELERATOR DESCRIPTION

Accelerating Structure and Electron Gun

We constructed standing wave linac using on-axis coupled accelerating structure operating at 2856 MHz. There are total 24 accelerating and 23 coupling cells in the linac. The first accelerating cell with low field level acts as a pre-buncher, distance to the next cell, the next two cells length and field strength were adjusted to provide > 60% capture efficiency, subsequent 21 accelerating cells have $\beta = 1$, the linac length is 1.24 m. On-axis electric field distribution measured for brazed structure is shown at Fig. 1. Accelerating structure coupling to waveguide after brazing was tuned to 2.8.
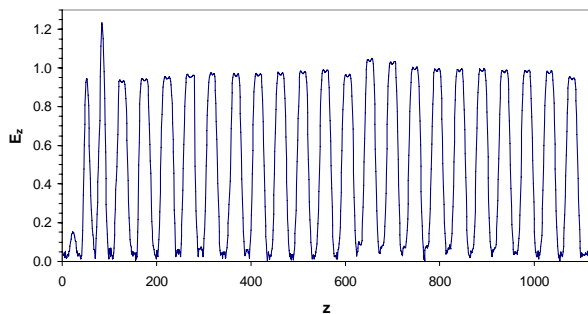

Figure 1: On-axis field distribution.

The nominal pulsed RF power dissipated in the

structure walls is 1.5 MW, so with a 6 MW klystron the pulsed beam current about 400 mA can be accelerated to 10 MeV.

Due to intensive cooling by ring channels made at cells periphery and by radial channels drilled in the cell webs our structure can operate with a duty factor up to 10%.

Three electrodes electron gun provides electron beam with current regulated by intermediate anode voltage between ~200 mA and ~1000 mA at 50 kV cathode voltage. High voltage pulse from a klystron modulator is used to feed the gun. Intermediate anode high voltage pulse is obtained from a high voltage divider regulated in discrete steps. The electron gun electrodes geometry was optimized to minimize beam dimension change with the beam current variation.

RF system

In our RF system klystron operates in auto-oscillation mode with an accelerating structure in the feed-back loop similar to our previous work [2]. The klystron oscillation frequency automatically follows to a drift of accelerating structure frequency, caused by different factors, so no additional frequency stabilization system is required. Moreover, because of a discharge in feeding waveguide or accelerating structure brakes the auto-oscillation conditions, at nominal beam current and energy (close to zero reflected wave at pulse top) a klystron can feed a standing wave linac without circulator.

Three types of klystrons with pulsed power 6 MW and average power 6 kW, 25 kW and 70 kW [3] can be used to get beam with maximum average power 4, 16 or 45 kW. Described below measurements of the beam parameters were conducted with the klystron KIU-168 with pulsed/average power 6 MW/6 kW.

BEAM PARAMETERS

Test Stand

Test stand is shown schematically in Fig. 2(a), its photo is given in Fig. 2(b). Electron gun current was controlled with a current transformer (3). To view the beam image we used transition radiation generated by the beam at a movable cooled screen placed in vacuum chamber (6). Transition radiation was registered by a CCD camera synchronized with the modulator; pulse to pulse beam images were stored at a computer. Beam energy spectrum was measured by a spectrometer consisting of 45° magnet (8), collimating slit (11) and beam collector (10). The spectrometer resolution defined by the magnet focusing properties and collimating slit width was $\pm 1\%$. The beam

current and power at 0° was measured with collector (9). Steering coils (5) were used to maximize beam transmission while a solenoid (4) adjusted beam focusing at a low beam energy mode of linac operation.

We conducted the measurements for different: (1) klystron maximum power, regulated by the modulator pulse high voltage amplitude; (2) the klystron output power regulated by a feed-back loop attenuation; (3) the gun current regulated by the intermediate anode voltage;

and (4) values of the solenoid field. Accelerating field level was controlled by RF signal from a probe installed in the accelerating cell connected with the feeding waveguide. The RF diode signal amplitude was calibrated with respect to RF power losses in the structure walls, calculated from the measured difference of inlet and outlet cooling water temperature and known water flow. Independent calibration of the RF diode was done with respect to a beam energy, measured by the spectrometer.
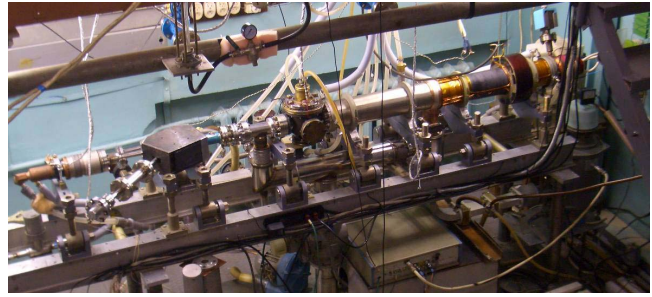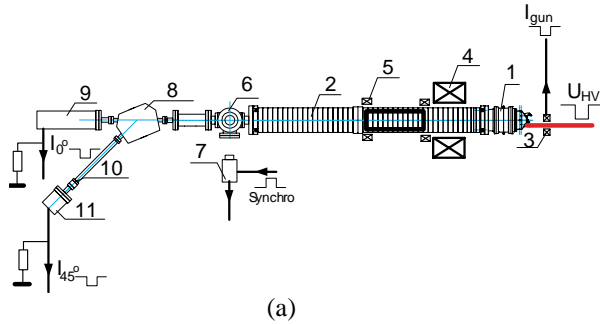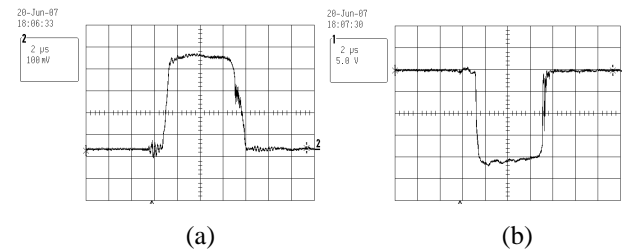

Figure 2: Test stand schematically (a) and photo (b). 1– electron gun, 2- accelerating structure, 3- beam current transformer, 4- solenoid, 5- steering coils, 6- chamber with movable cooled screen, 7- CCD camera, 8- 45° bending magnet, 9, 11 – beam collectors, 10- collimating slit.

Results

In Fig. 3 we show RF probe (a) and beam current (b) signals registered for beam energy 10 MeV and pulsed current 430 mA. The pulse length ~6.3 µs is defined by the modulator high voltage pulse duration.

Figure 3: RF probe (a) and beam current (b) signals.

Figure 4: Dependence on high voltage pulse amplitude of (a) pulsed beam current and (b) capture efficiency.

Pulsed accelerated beam current dependence on the high voltage pulse amplitude is shown in Fig. 4 (a). By changing the high voltage pulse amplitude we changed the klystron output RF power $\sim U_{kl}^{5/2}$ and the gun current

$\sim U_{kl}^{3/2}$ because of the gun is fed from the klystron modulator. To decrease reflected RF power by increasing the beam loading, at $U_{kl} = 45$ kV an intermediate anode voltage was increased 1.36 times by switching high voltage divider, thus increasing gun current about 1.6 times. These measurements were conducted with focusing solenoid switched off.
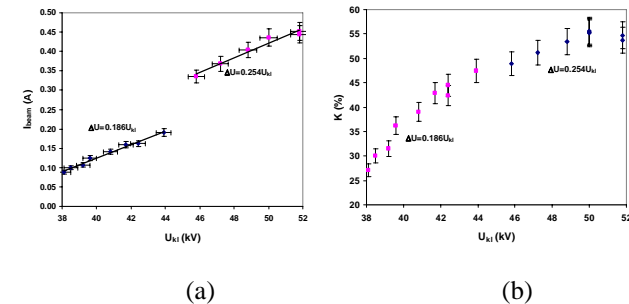
In Fig. 4(b) capture efficiency (ratio of accelerated beam current to gun current) is shown. When approaching nominal operational parameters the capture efficiency is approaching to theoretical value ~60%.
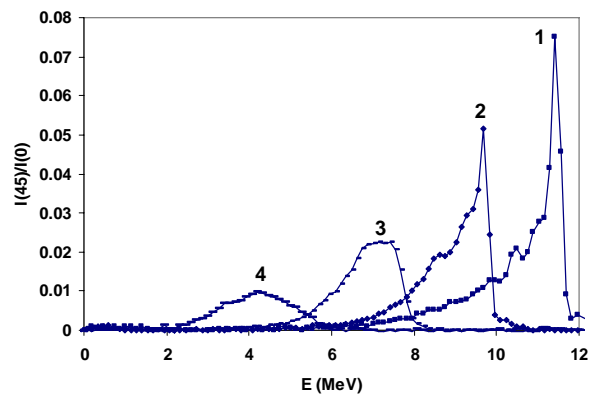

Figure 5: Beam energy spectra.

An output beam energy adjustment is important for some applications. We regulated beam energy by changing the RF feed-back loop attenuation. In this way we changed the klystron output power and so the accelerating field level. We found focusing solenoid current providing maximum capture efficiency at lowest

beam energy and conducted all measurements with this current. The focusing solenoid field within achieved regulation range did not influence on the capture efficiency at highest beam energy.

Beam energy spectra measured for the klystron voltage in the range 52 – 54 kV and for the gun current about 700 mA are shown in Fig. 5. As one can see, we are able to regulate the energy of the spectrum maximum from ~11.5 MeV to ~4 MeV. The width of the energy spectra at low energy is defined mainly by the beam dynamics effects – slippage of the beam phase with respect to RF field phase, while at high energy it is connected mainly with the RF pulse top unflatness, especially near the pulse edges.

We should note that when regulating beam energy by changing klystron output power with constant high voltage amplitude and constant gun current, we have different reflected RF power at different energies. This reflected power without a circulator returns back to the klystron and influences on the level of generated RF power. To remove this influence and to make klystron operation more safe, for the linac with regulated beam energy a circulator must be installed at the klystron exit.

In Fig. 6 a single shot beam images obtained at 15 cm from the linac exit are shown for high and low output energies. Both images were obtained at the same solenoid current 6A, rms beam radii are ~1 mm in both cases.
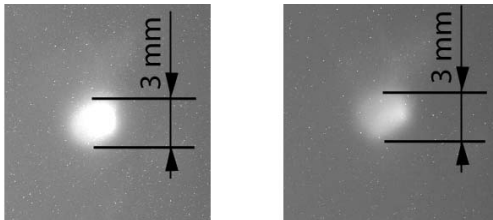

Figure 6: Single shot beam image, ~10 MeV, left and ~5 MeV, right. Solenoid current 6 A.

Comparison with calculations

Global parameters of linac operation such as RF power dissipated in the structure walls for nominal beam energy, beam power and capture efficiency are in good correspondence with theoretical estimations. The parameter more sensitive to accuracy of beam dynamics calculations is rms beam radius at accelerator exit.
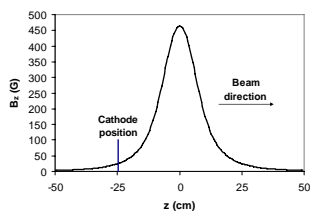

Figure 7: Solenoid field on linac axis at 10 A.

In Fig. 7 we show solenoid field distribution on the linac axis for the coil current 10 A. Field penetrates to the electron gun and its value at cathode is about 27 G for

10 A. Beam dynamics calculations taking into account this field were done with EGUN [4] and PARMELA [5] codes using SUPERFISH [6] fields. In Fig. 8 comparison of the measured and calculated rms beam radii at linac exit are presented in dependence on solenoid current for nominal beam energy and gun current 800 mA. Registered by CCD camera and calculated beam images at 15 A are given at Fig. 9.
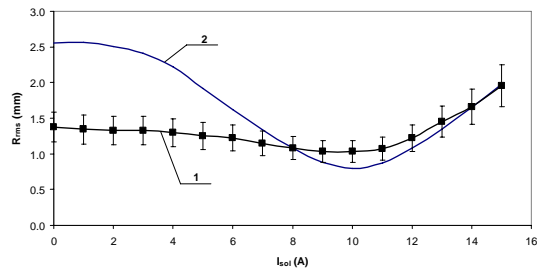

Figure 8: Rms beam radius dependence on solenoid current at 10 MeV: (1) – measured, (2) - calculated.
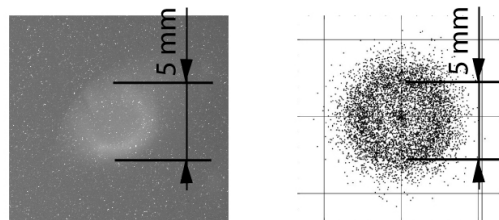

Figure 9: Registered by CCD camera and calculated beam images at 15 A.

Qualitative agreement between calculated and measured radii dependence on solenoid current is rather good. Annular beam form clearly seen with CCD camera above 12 A (see Fig. 9) is reproduced in calculations, it appears only with magnetic field at gun cathode switched on. At low solenoid current calculated radii exceed measured about 1.8 times, beam image has horizontal/vertical asymmetry and is skewed. This can be explained by effect of coupling slots and coupling widow generating quadrupole and skewed quadrupole fields.

REFERENCES

[1] A.V. Grizlov, V.N. Iliin, S.V. Lamonov et al., Proc. the XI Int. Conf. on Charged Particle Accelerators Applied in Medicine and Industry, St. Petersburg, Russia, October 10-14, 2005, p. 132

[2] A.N. Ermakov, D.I. Ermakov, B.S. Ishkhanov et al, , Instr. and Exp. Tech., Vol. 45, No. 4 (2002) 482

[3] I.A. Frejdovich, P.V. Nevsky, V.P. Sakharov et al, IVEC-IVESC 2006 Proceedings, April 25 – 27, 2006, Monterey, CA 93940, Report N13.5

[4] W.B. Herrmannsfeldt, SLAC-PUB-2631

[5] PARMELA - originally developed by K.R. Crandall

[6] SUPERFISH Reference Manual, LA-UR-87-126